FLUID DYNAMICS OF VITRECTOMY PROBES

TOMMASO ROSSI, MD,* GIORGIO QUERZOLI, PHD,† GIAMPIERO ANGELINI, DENG,‡
CARLO MALVASI, DENG,‡ MARIO IOSSA, MD,* LUCA PLACENTINO, MD,* GUIDO RIPANDELLI, MD§

Purpose: To characterize the fluidics of vitreous cutter port in response to aspiration and blade motion using particle image velocimetry techniques. Diverse surgical scenarios and fluid characteristics were replicated.

Methods: The 23-gauge vitreous cutters were immersed in seeded Balanced Salt Solution (BSS) (Alcon, Forth Worth, TX) or egg albumen, and high-speed video was recorded. Fluid velocity, kinetic energy (KE), and acceleration generated by Venturi and peristaltic pumps were measured in *aspiration only* (200 and 300 mmHg), *low-speed* vitrectomy (1,600 cuts per minute; 200 mmHg vacuum), and *high-speed* vitrectomy (3,000 cuts per minute; 300 mmHg vacuum) modes.

Results: The Venturi pump generated significantly higher KE than peristaltic pump in BSS ($P < 0.0001$ for each pair), and *aspiration only* yielded significantly higher KE. Cutting activation generated significant acceleration ($P < 0.001$), and the peristaltic pump produced higher positive and negative acceleration peaks ($P < 0.001$) than the Venturi pump. In egg albumen, the peristaltic pump generated significantly more KE than the Venturi pump ($P < 0.001$) and perturbed a much wider area. Acceleration was higher for the peristaltic pump in *low-speed* mode ($P < 0.001$), whereas in *high-speed* modality, the Venturi pump produced the highest acceleration peaks ($P < 0.001$).

Conclusion: Pump type and blade motion largely influence velocity, KE, and acceleration. In BSS, the Venturi pump induces higher KE and acceleration, although perturbing fluid less diffusely. In egg albumen, the peristaltic pump perturbed a much wider area and induced a higher KE and acceleration than the Venturi pump, even more so at lower cut rates. As a conclusion, particle image velocimetry allowed precise characterization of fluid velocity in response to cutter activation, suggesting a pragmatic approach to surgical scenarios.

RETINA 34:558–567, 2014

Since the introduction of vitrectomy,[1] researchers and surgeons have strived to improve the efficacy and safety of vitreous cutters. While most improvements pointed in the direction of gauge reduction and cut-rate increase,[2] the understanding of cutter fluidics did not progress accordingly.

The vitreous is a nonnewtonian fluid with uneven viscosity and fibril structure, and its removal through small-gauge probes is technically challenging and potentially dangerous because of the presence of unpredictable, localized retinal adhesion. An accurate comprehension of vitreous perturbation in response to suction and blade motion is essential for the improvement of vitrectomy probes.

Particle image velocimetry (PIV) is a well-known image analysis technique[3] that allows statistical computation of fluid motion patterns also in the presence of high levels of noise[4] and has been previously applied to ophthalmology.[5]

The purpose of the present article is to study vitreous cutter port fluidics under diverse surgical scenarios, by means of PIV: "low-speed" and "high-speed" settings with Venturi and peristaltic pumps have been tested to speculate on the biologic effects and surgical relevance of fluid flow rate, kinetic energy (KE), and acceleration.

From the *Eye Hospital of Rome, Rome, Italy; †Department of Civil and Environmental Engineering and Architecture, University of Cagliari, Caligari, Italy; ‡Optikon 2000 Inc., Rome, Italy; and §G.B. Bietti Foundation for Study and Research in Ophthalmology Research Hospital, Rome, Italy.

G. Angelini and C. Malvasi are employees of Optikon 2000 Inc. None of the other authors have any financial/conflicting interests to disclose.

Reprint requests: Tommaso Rossi, MD, Via Tina Modotti, 93, Rome 00142, Italy; e-mail: tommaso.rossi@usa.net

Materials and Methods

Experimental Setting

To simulate *aspiration only*, *low-speed*, and *high-speed* vitrectomy modes, 23-gauge vitreous cutters were connected to a vitrectomy machine console (R-Evolution; Optikon 2000, Inc, Rome, Italy) equipped with double Venturi/peristaltic pump and then tested under various combinations of T1 cut rate and aspiration settings (Table 1). The vitreous cutters were secured vertically with the distal 20-mm probe tract immersed in a transparent Plexiglas box ($3 \times 5 \times 3$ cm parallelepiped) filled with Balanced Salt Solution (BSS) (Alcon, Forth Worth, TX) or egg albumen[6] to investigate aqueous fluidics and the behavior of a vitreous analogous with fibril structure.[7]

To allow optical PIV tracking, BSS was injected with 0.2 mL of triamcinolone crystals (Kenacort; Bristol Myers-Squibb, Princeton, NJ), whereas egg albumen was seeded with air microbubbles. Triamcinolone vials were aspirated through a 40-μm filter, to remove particle macroaggregates.

A 2-mm-wide vertical slit of light was shined directly onto the cutter port from a sidewall of the Plexiglas box to minimize light scattering from areas distant from the cutter shaft plane. The camera was positioned 90° away from the light source and focused on the plane of the vitreous cutter port that was oriented directly toward the light (i.e., at 90° from the camera view) (Figure 1).

High-Speed Imaging

Fluid motion around the vitreous port was recorded for 2 consecutive seconds with MotionPro high-speed camera (Integrated Design Tools, Inc, Tallahassee, FL) and stored as uncompressed audio–video interleaved format (.avi) movies (frame rate was 1,000 frames per second, and resolution was $1,024 \times 1,280$ pixels). Five seconds were allowed between vitreous cutter onset and video recording, to skip the transitional phase.

Table 1. Vitreous Cutter Settings: Both the Venturi (V) and Peristaltic (P) Pumps Were Used in All Tests With Suction and Cut Rate Set at Typical "Low-Speed Vitrectomy" and "High-Speed Vitrectomy" Combinations

Modality	Cut Rate (cpm)	Aspiration (mmHg)	Pump (Venturi, Peristaltic)
Aspiration 1	0	200	V and P
Aspiration 2	0	300	V and P
Low speed	1,600	200	V and P
High speed	3,000	300	V and P

The peristaltic pump was set at a flow rate of 15 mL/minute in all cases.

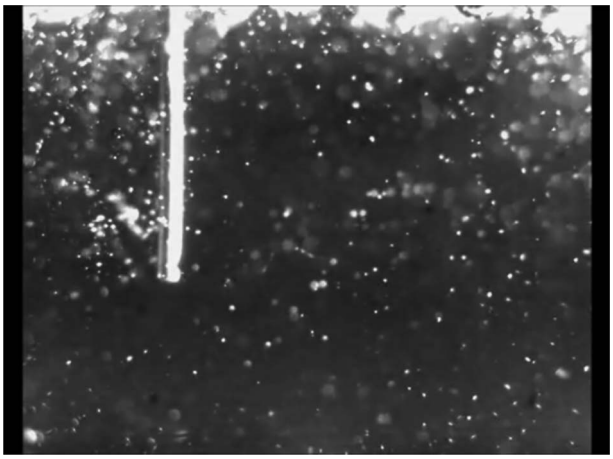

Fig. 1. Measure setting snapshot. The cutter probe is immersed in fluid (BSS or egg albumen) seeded with triamcinolone crystals (BSS) or air microbubbles (egg albumen) to improve streamline visualization and record. A slit of light is projected directly onto the cutter port 90° away from the camera view. The port is oriented toward the light source.

Particle Image Velocimetry

Particle image velocimetry measures fluid velocity from high-speed movies by recognizing the motion of tracers dispersed in the working fluid (i.e., triamcinolone crystals or microbubbles). Under the assumption that tracers translate in subsequent frames conserving their brightness, corresponding windows on the successive images are compared. The displacement minimizing the dissimilarity between the corresponding windows is assumed to be representative of fluid motion in that region. For image analysis, we used robust imaging velocimetry, as elsewhere applied to ophthalmology.[5] Compared with the classical PIV algorithm, robust imaging velocimetry uses a measure of dissimilarity, which is statistically robust to outliers and therefore less affected by noise, artifacts, or velocity gradients within the interrogation window.[8]

Velocity Measures—Main Outcome Measures

To obtain a global measure of the fluid motion, irrespective of velocity vector orientation, the mean KE of a given perturbed fluid volume around the cutter port was considered. Kinetic energy has been defined as the spatial average at a given instant of the local KE per unit mass (i.e., $1/2\ V^2$; where V = velocity). The considered "perturbed area" included a $1,024 \times 1,280$ pixel window ($20 \times 8 \times 26$ mm). When the cutter was on, given the periodicity of fluid perturbation, KE was phase averaged on multiple sample cycles, to improve data robustness (25 cycles at 1,660 cuts per minute [cpm] and 50 cycles samples at 3,000 cpm). Conversely, when the cutting was off, KE data were low-pass filtered to cut noise.

Acceleration was derived from velocity measures and calculated as variation per unit time of the square root KE. Data were processed by phase averaging and filtering as above.

Spatial maps of velocity magnitude have been developed based on the velocity measures obtained through robust imaging velocimetry. Two different types of spatial maps have been shown: an "average" map in which velocity is averaged throughout the 2 seconds of registration and an "peak" map in which the highest calculated velocity value is shown.

Statistical Analysis

Testing the significance of curve difference poses peculiar problems, and several techniques have been proposed.[9] Given the surgical relevance of both general fluid behavior and instantaneous conditions, we elected to compare separately peak values and entire curves.

Kinetic energy and acceleration peak (both positive and negative) values have been compared by means of paired *t*-test, whereas overall curve behavior was evaluated through the area under the curve (AUC) comparison and used chi-squared test. Significance (*P*) has been set at the 0.05 level in all cases.

Results

BSS KE curves are reported in Figure 2 for *aspiration only 1 and 2*, *low-speed*, and *high-speed* vitrectomy modes, using the peristaltic and the Venturi pumps. The Venturi pump determined significantly higher KE than the peristaltic pump ($P < 0.0001$ for each pair; Figure 2, A and B) and *aspiration only 1 and 2* modality yielded significantly higher KE than *low-speed* and *high-speed* vitrectomy modalities, regardless of pump modality and aspiration regimen ($P < 0.0001$ for each pair; Figure 2, C and D).

Both "aspiration only" settings in egg albumen resulted in cutter port jamming soon after start and have not been reported. *Low-speed* and *high-speed*

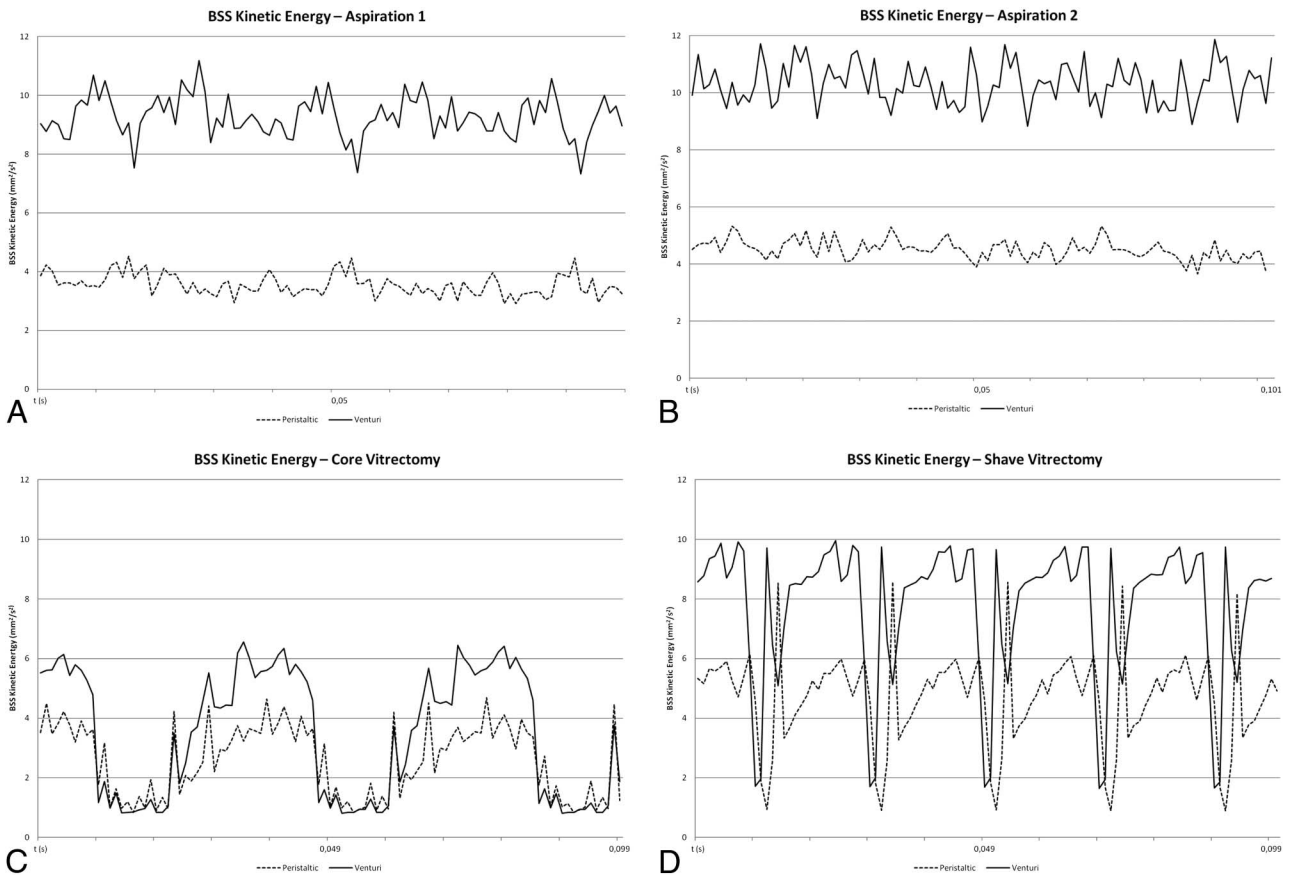

Fig. 2. Kinetic energy curves in BSS. **A.** *Aspiration only 1* mode at 200 mmHg vacuum. **B.** *Aspiration only 2* mode at 300 mmHg vacuum. **C.** *Low-speed* mode at 1,600 cpm and 200 mmHg vacuum. **D.** *High-speed* mode at 3,000 cpm and 300 mmHg vacuum. Significant decrease in KE is noted once cutting is engaged, and the strict correlation between blade motion and KE variations is also observed. Cut rate can actually be derived from KE behavior that clearly shows 3 cycles (in 0.1 second) at 1,600 cpm and 5 cycles (in 0.1 seconds) at 3,000 cpm. Venturi pump resulted in significantly higher KE in both *low-speed* and *high-speed* mode.

KE curves in egg albumen are reported in Figure 3: the peristaltic pump generated significantly more KE than the Venturi pump in both *low-speed* and *high-speed* modes and much higher KE peak values than the corresponding BSS values ($P < 0.001$ for each pair). The peristaltic pump resulted in significantly higher peak KE values when a lower cut rate (i.e., 1,600 cpm and 200 mmHg at *low-speed* setting; Figure 3A) was used, compared with higher cut rate (i.e., 3,000 cpm and 300 mmHg at *high speed*; $P < 0.001$) with the same pump (Figure 3A vs. Figure 3B, dashed line).

Color maps of velocity magnitude are reported in Figures 4–7, for BSS and egg albumen, respectively. Average velocity spatial maps of BSS (Figure 4) show a significantly larger perturbed area and higher velocities as suction increases (Figure 4, C and D vs. Figure 4, A and B). The Venturi pump yields higher velocity than the peristaltic one at comparable vacuum (Figure 4B vs. Figure 4, A and D vs. Figure 4C). Average velocity spatial maps of egg albumen (Figure 6) showed much lower velocity and erratic streamlines when suction is obtained through the Venturi pump, whereas maps obtained with the peristaltic pump exhibited perturbations propagating to large distances along some preferential path. This is particularly apparent with the *high-speed* settings (Figure 6C), where streamlines confirm the presence of a stable preferential path toward the port. The decrease in velocity recorded within the immediate proximity of the port noted in Figure 6, A and C is to be ascribed to particle image disappearance within the port itself and out of the measuring range, thus simulating deceleration with current video recording frame rate. "Peak" velocity spatial maps show much higher velocities and a wider perturbed field, both in BSS (Figure 5) and in egg albumen (Figure 7).

Acceleration curves in BSS are reported in Figure 8. Both *aspiration only* settings resulted in low accelerations, and the difference between overall curve behaviors with peristaltic and Venturi pumps did not reach statistical significance neither at 200 mmHg (*aspiration only 1*; Figure 8A) nor at 300 mmHg level (*aspiration only 2*; Figure 8B). Interestingly, acceleration fluctuation at *aspiration only 1* (200 mmHg) was greater than at *aspiration only 2* (300 mmHg) with both pumps.

In *low-speed* modality (1,600 cpm and 200 mmHg; Figure 8C), acceleration attained much higher peak (both positive and negative) values than in *aspiration only 1 and 2* modalities ($P < 0.001$ in both pairs). Specifically, the peristaltic pump produced significantly higher positive and negative acceleration peaks ($P < 0.001$) than the Venturi pump. Acceleration AUC did not reach statistical significance in *low-speed* modality. At higher cut rates (*high speed*: 3,000 cpm and 300 mmHg; Figure 8D), neither peak values nor overall curve behavior (as measured by means of the AUC) differed significantly between the pumps.

Acceleration curves in egg albumen (Figure 9) produced significantly higher peak for the peristaltic pump at lower cut rates (*low speed*: 1,600 cpm and 200 mmHg; $P < 0.001$ for each pair; Figure 9A), while at *high-speed* settings (3,000 cpm and 300 mmHg), the Venturi pump produced the highest acceleration peaks ($P < 0.001$ for each considered pair).

Discussion

Vitreous cutter evolution led to probe gauge reduction and cut-rate increase, reducing port-related complications[10] and improving patients' comfort and recovery speed.[11] However, a better understanding of cutter fluidics remains mandatory for safer vitrectomy

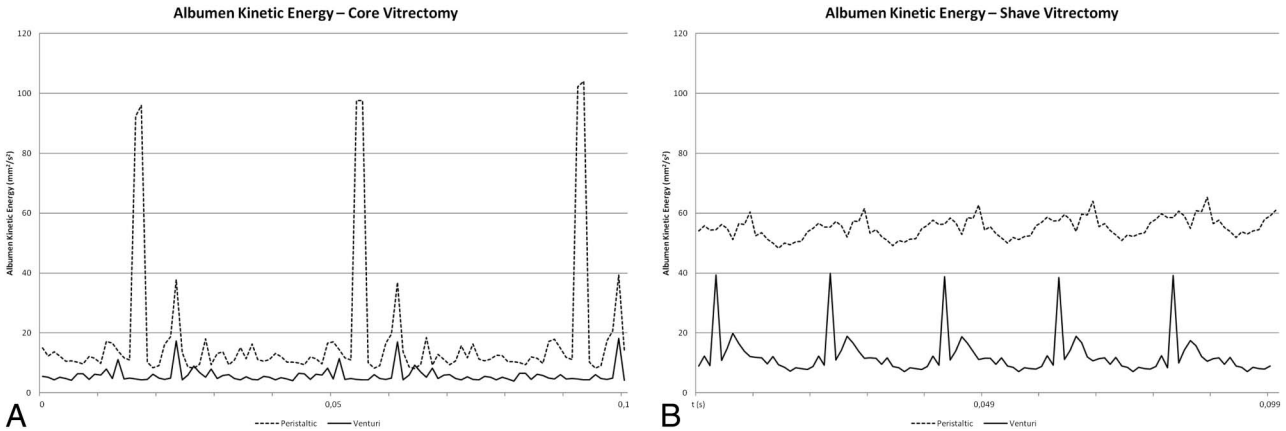

Fig. 3. Kinetic energy curves in egg albumen: *low speed* modality (**A**) and *high speed* modality (**B**). Interestingly, the peristaltic pump (dashed line) determines significantly higher KE levels and peaks in both cases. It is noted that lower cut rates allow a much higher peak KE with the peristaltic pump.

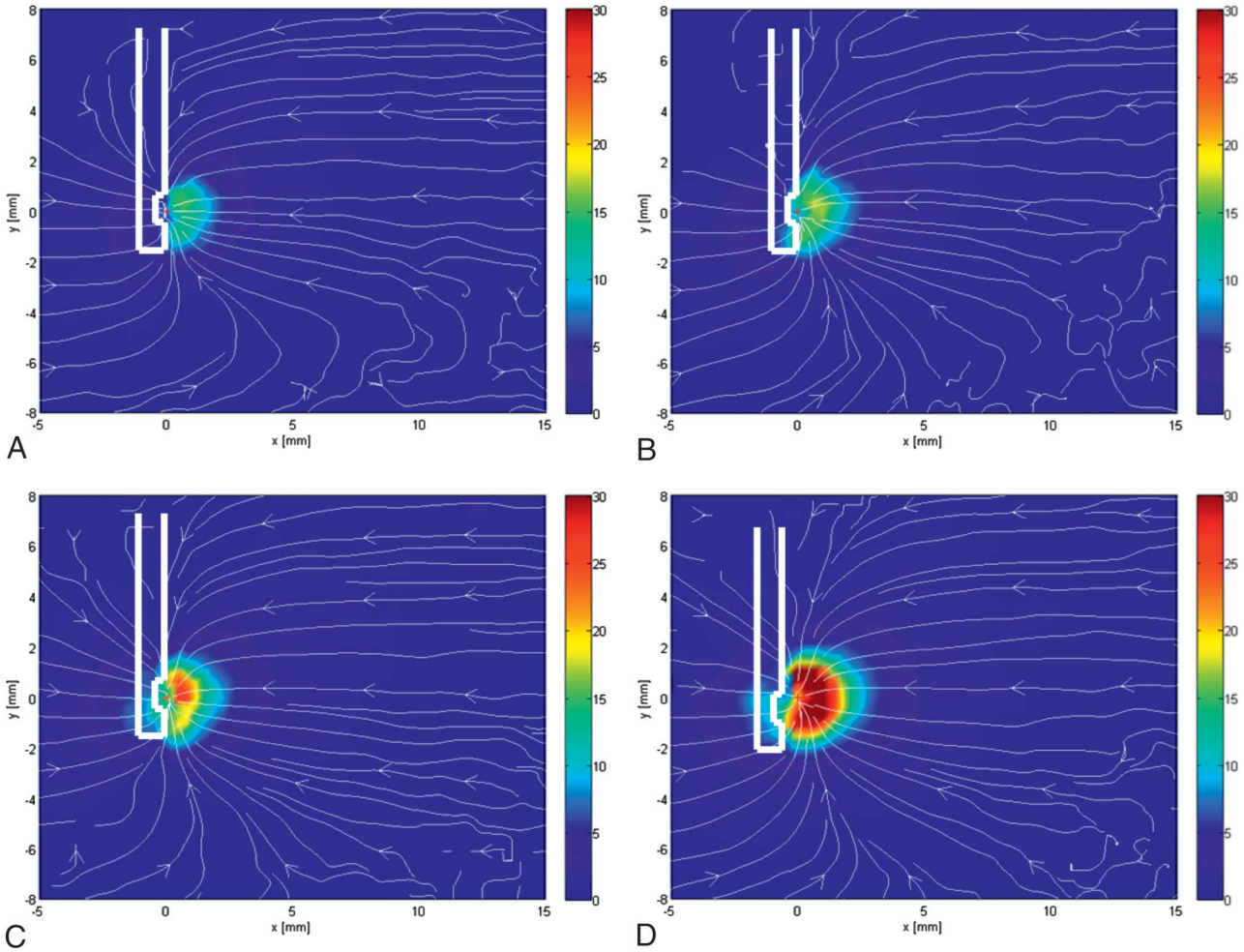

Fig. 4. Spatial map of the "average" velocity in BSS in *low-speed* (**A** and **B**) and *high-speed* (**C** and **D**) vitrectomy modes with peristaltic (**A** and **C**) and Venturi (**B** and **D**) pumps. Colors indicate velocity (millimeters/second) according to the right bar, *x* and *y* axes space (in millimeter), and origin ($x = 0$; $y = 0$) is the vitreous cutter port, where a schematic cutter draw with port facing rightward has been added. The streamlines of the velocity field are drawn in white. They are representative of the path that fluid follows, on average, while approaching the port. Increase in suction determines an increase in fluid velocity, more evident with the Venturi pump. The streamlines are clearly evident and predictably point toward the cutter port. The perturbed area around the port is limited to a 2-mm to 3-mm radius, and extremely low velocity can be detected further away.

and a prerequisite for the development of more efficient probes.[12]

While previous studies focused on flow rate,[13] vitreous mass removal,[14] and retinal traction measures,[15] the present study introduces PIV as an objective means of analyzing fluid perturbation in response to aspiration and blade motion. Venturi and peristaltic pumps have been tested under typical surgical scenarios: a *low-speed* vitrectomy and a *high-speed* modality (Table 1).

Pump type largely influenced KE: Venturi pump induced higher BSS energy than the peristaltic pump, regardless of vacuum level and vitrectomy modality (Figures 2 and 3). When cutting was activated (Figure 2, C and D), KE became entirely dependent on blade motion, increasing right after the port opened and decreasing abruptly when the port closed. Although the surgical relevance of traction exerted by cutter vacuum on the retina in BSS is often considered negligible,[16] it is essential whenever the retina detaches and fluid acceleration threatens to engage it with every blade cycle.[17] This is evident in Figures 4 and 5, where spatial maps show abrupt KE rise in the immediate proximity of the port but cannot be considered negligible even 180° away from it. Therefore, the development of safer cutters should consider minimizing low viscosity fluid acceleration to reduce the risk of untoward retinal entrapment, especially when both vitreous and aqueous are present at the same time and sudden suction rise, more common.

In egg albumen (Figure 3), the peristaltic pump induced higher KE than the Venturi pump. In particular, "low speed" produced similar average KE but with higher KE peaks (Figure 3A), whereas *high speed*

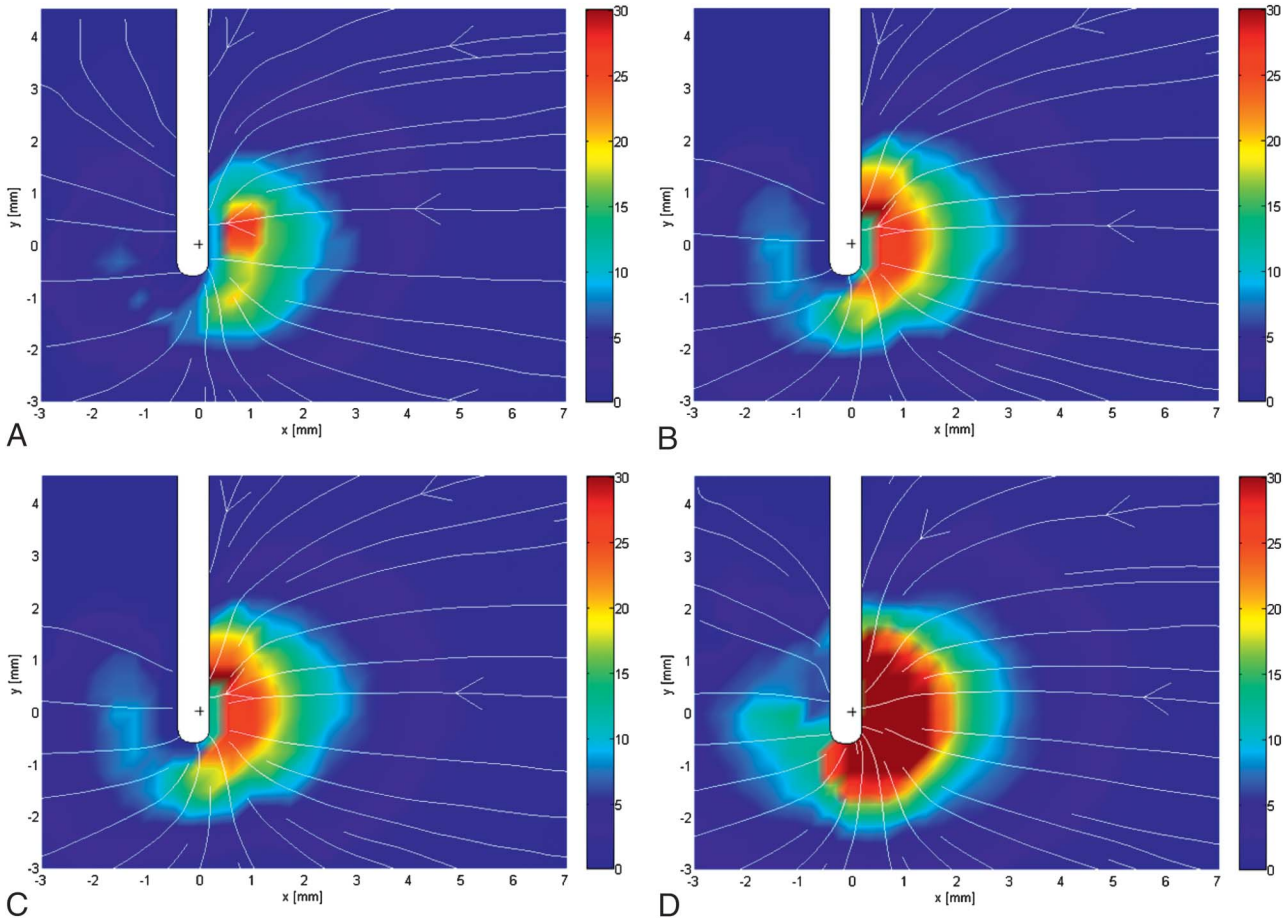

Fig. 5. Spatial map of "peak" fluid velocity in BSS in *low-speed* (**A** and **B**) and *high-speed* (**C** and **D**) vitrectomy modes with peristaltic (**A** and **C**) and Venturi (**B** and **D**) pumps. Colors indicate velocity (millimeters/second) according to the right bar, *x* and *y* axes space (in millimeter), and origin ($x = 0$; $y = 0$) is the vitreous cutter port. The cutter is held vertically from top to bottom, and the port is facing rightward. Velocities are distributed throughout a wider area and reach higher intensity than that showed in Figure 4.

determined a higher average KE with less pronounced peaks (Figure 3B). We believe that egg albumen fibril structure, similarly to vitreous, is responsible for this behavior more than viscosity. Peristaltic pumps, in fact, work by generating a pressure gradient required to maintain a constant flow rate, whereas Venturi pumps keep a constant pressure gradient, resulting in decrease in flow rate when additional resistance caused by egg albumen fibril structure is encountered.

The comparison of *high-speed* and *low-speed* settings with peristaltic pump (dashed lines in Figure 3) suggests that higher cut rates results in a more continuous flow probably because frequent cutting ease the removal of smaller chunks of fibril material. It should be noted that peristaltic pumps build up vacuum even when the port is closed; also, pressure gradient increases while the blade obstructs the port completely and generates a sudden peak of KE as soon as the port opens.

When egg albumen is drawn into the port by suction and "stretched," KE propagates around the probe through the fibrils, regardless of viscosity; once the blade closes the port, fibrils are severed and traction released. Because lower cut rates allow a longer time in between 2 consecutive cuts, a constant volume-controlled pump (i.e., peristaltic pump, Figure 3, dashed line) engages fluid until occlusion occurs or a given volume is removed and vacuum builds up to a much higher level than allowed by a pressure-controlled pump (i.e., Venturi pump; Figure 3, continuous line).

Acceleration measures fluid velocity variation per unit time and is a reliable indicator of the forces induced on the retina by the time variability of suction per unit mass, as inertial force equals mass times acceleration ($F = m \cdot a$).

Blade activation determined a 5-fold increase in BSS acceleration (compared with *aspiration only 1 and 2*; see Figure 8, C and D vs. Figure 8, A and B) and clearly beat the pace of port closure, whereas pump type did not significantly influence acceleration.

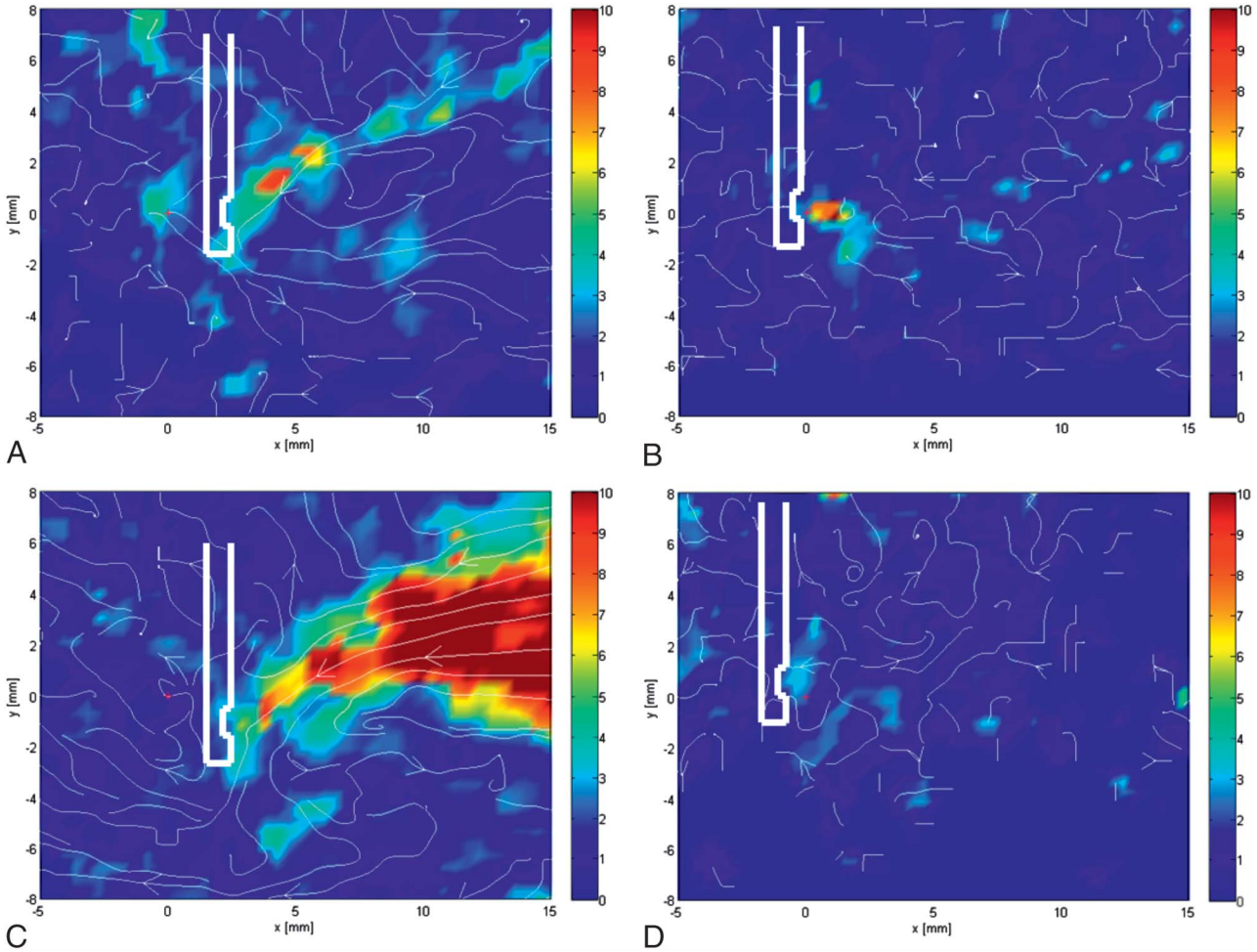

Fig. 6. Spatial map of the "average" fluid velocity in egg albumen in *low-speed* (**A** and **B**) and *high-speed* (**C** and **D**) vitrectomy modes with peristaltic (**A** and **C**) and Venturi (**B** and **D**) pumps. Colors indicate velocity (millimeters/second) according to the right bar, *x* and *y* axes space (in millimeters), and origin ($x = 0$; $y = 0$) is the vitreous cutter port. The cutter is held vertically from top to bottom, and the port is facing rightward. Velocities are distributed throughout a much wider area, and streamlines are a lot more complex than those designed in BSS. Measures obtained with peristaltic pump (**A** and **C**) reveal much higher velocities than those obtained with the Venturi pump (**B** and **D**). The perturbed area around the vitreous cutter port is significantly wider in albumen than in BSS (Figure 3) and extends well over 10 mm to 15 mm, that is, almost the vitreous chamber span.

Things changed in egg albumen (Figure 9): acceleration more than doubled with the Venturi pump and rose of almost an order of magnitude (≈8 times) with the peristaltic pump in *low-speed* modality (compare Figures 7A and 6C). The *high-speed* modality, working at higher cut rates, determined much higher acceleration when the Venturi pump was used. Teixeira et al[18] measured traction exerted on a strain gauge transfixed through the retina in pig eyes and found a direct relation between vacuum and traction, whereas cut rate increase decreased force.

Acceleration data seem to suggest meaningful surgical tips: the removal of a fibril structured viscous fluid (such as young, "formed" vitreous) generates less traction if performed at higher cut rates (*high-speed* mode) and peristaltic pumps reduce traction, especially when working closer to the retina. Conversely, a Venturi pump allows a gentler *low-speed* vitrectomy under the same fluid physical conditions. The extent of KE propagation is also extremely important, especially in cases such as vitreomacular traction syndromes or impending macular holes when "remote" vitreoretinal adhesions at sensitive locations such as the macula may condition the prognosis. The fibril structure of vitreous, in fact, as well as egg albumen (see spatial map, Figures 6 and 7), transmits KE and acceleration far away from the cutter tip, and the reducing KE and acceleration limits undue traction.

Syneretic vitreous, such as those in older patients or after PVD, on the contrary, would behave much like BSS and suggests different cutter parameters: the Venturi pump would prove more efficient even at higher cut rates and acceleration difference would not be clinically significant (Figure 8, C and D).

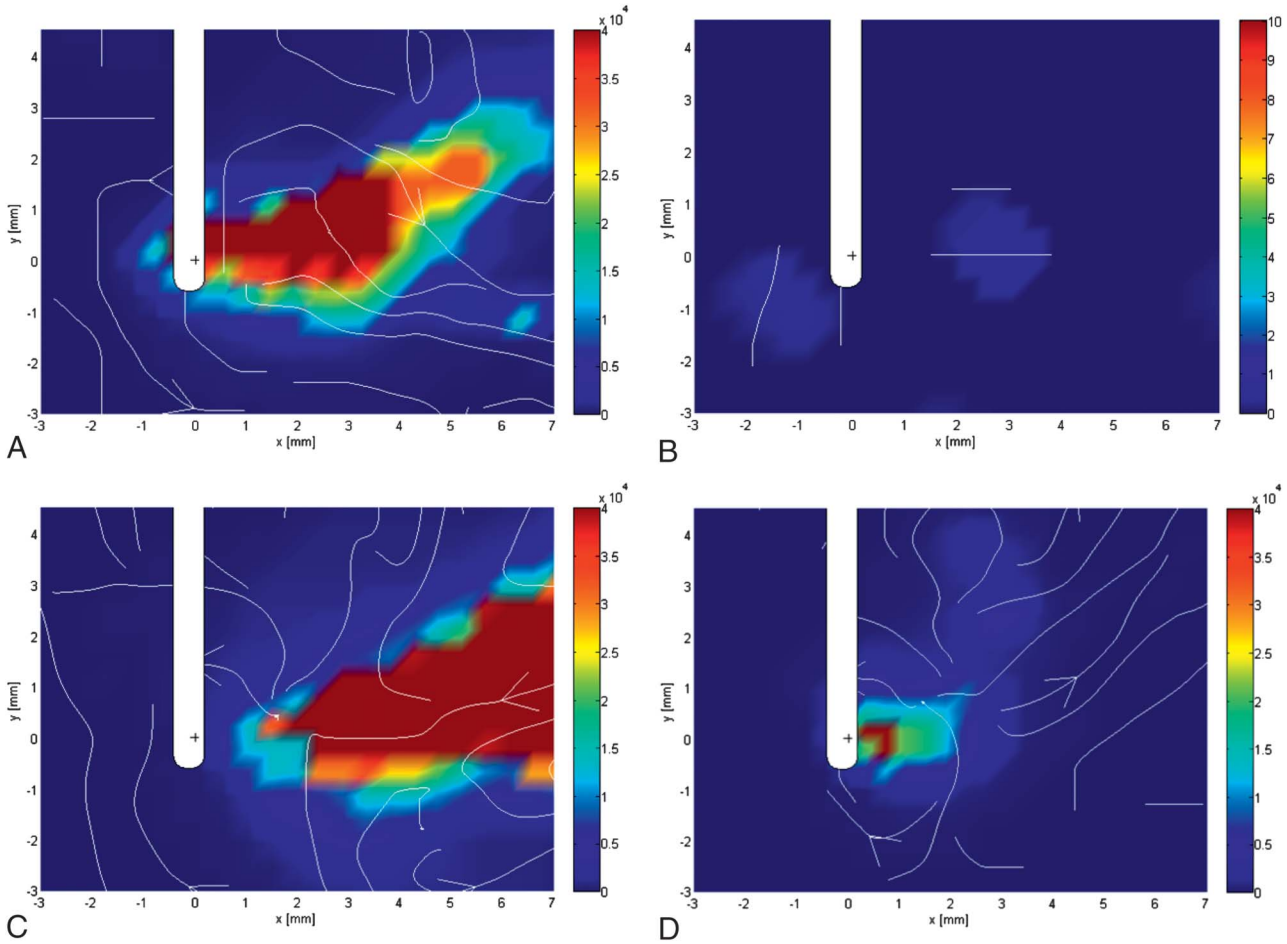

Fig. 7. Spatial map of the "peak" fluid velocity in egg albumen in *low-speed* (**A** and **B**) and *high-speed* (**C** and **D**) vitrectomy modes with peristaltic (**A** and **C**) and Venturi (**B** and **D**) pumps. Colors indicate velocity (millimeters/second) according to the right bar, *x* and *y* axes space (in millimeters), and origin ($x = 0$; $y = 0$) is the vitreous cutter port. The cutter is held vertically from top to bottom, and the port is facing rightward. Peak velocities do not show a clear-cut increase in velocity as a result of the fibril structure that propagates motion much longer than water.

Spatial maps greatly help visualize medium response to cutter functioning: BSS (Figures 4 and 5) responded as expected to suction and blade motion, increasing velocity as the fluid approached the cutter port and streamlines predictably pointed toward the port lumen from all direction; the perturbed area increased as a direct function of suction, and the Venturi pump proved more efficient. On the contrary, the intrinsic structure of egg albumen (Figures 6 and 7) diffused energy unpredictably and the peristaltic pump perturbed a much wider area, as big as the entire vitreous chamber, where wave reflection and amplification should also be taken into account, complicating our task exponentially. Based on these maps, it should be noted that the fluid volume interested by the cutter-induced perturbation is at least as big as the entire vitreous chamber before even considering reflections.

Several explanations could account for such phenomenon: the fibrils may simply transmit energy remotely, as an elastic medium, showing much less damping capability than a newtonian fluid. Fibrils also tend to interact with the flow deforming and reorientating so as to create a sort of "channel of drainage," that is, preferential paths for the incoming fluid. Once a channel is conformed, the fluid would follow the same path because the fibrils do not rearrange in a new configuration. Therefore, KE is not diffused in all direction evenly (as with BSS) but is restricted to the "channels," where it tends to attain high values also far from the port. This "unpredictable" diffusion of velocity in egg albumen is probably the reason why peak spatial maps in egg albumen do not return the highest velocity pattern (compare Figure 7 with Figure 6), unlike BSS spatial maps (compare Figure 5 with Figure 4).

The present study introduces PIV as a novel way of studying vitreous perturbation in response to vitrectomy and has many pitfalls, typical of pilot studies. Definitely the choice of "low-speed" and "high-speed" parameters is arbitrary, and different surgeon may disagree or have different personal settings, as well as a preference

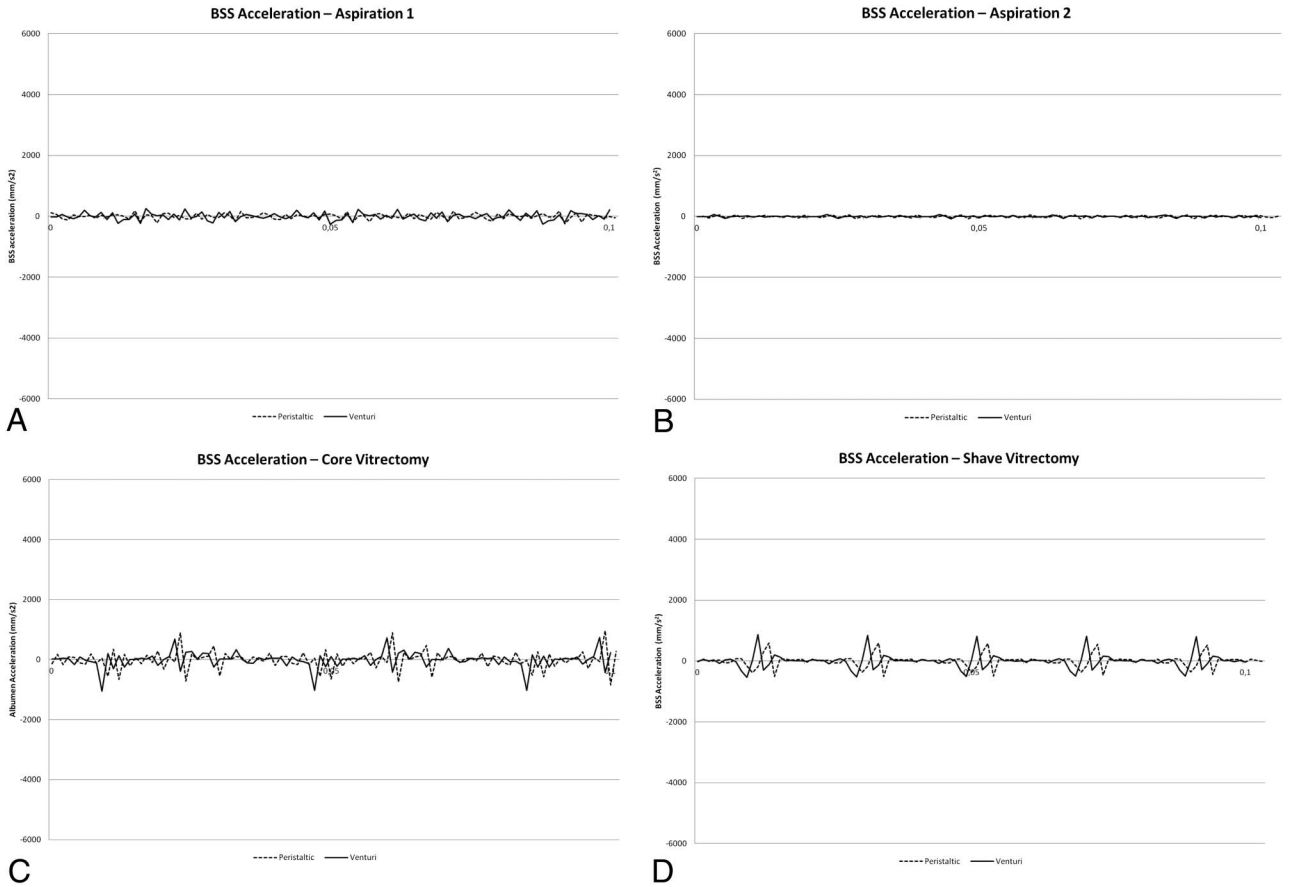

Fig. 8. Acceleration in BSS. **A.** *Aspiration only* mode at 200 mmHg vacuum. **B**. *Aspiration only* mode at 300 mmHg vacuum. **C.** *Low-speed* mode at 1,600 cpm and 200 mmHg vacuum. **D.** *High-speed* mode at 3,000 cpm and 300 mmHg vacuum. Acceleration is negligible until cutting is engaged and the port intermittently closed at a varying pace. In BSS (**A** and **B**), the two pumps showed no significant difference but a trend toward higher acceleration with the peristaltic pump at lower cut rates and the opposite in *high-speed* mode.

toward different vitrectomy machines with varying technical specifications. Although we acknowledge this limitation, we intentionally used one single machine among the very few, allowing double pump technology to exclude biases related to pump control software. Surgical parameters may also vary among surgeons, although those that have been tested can be considered representative of different surgical times and purposes.

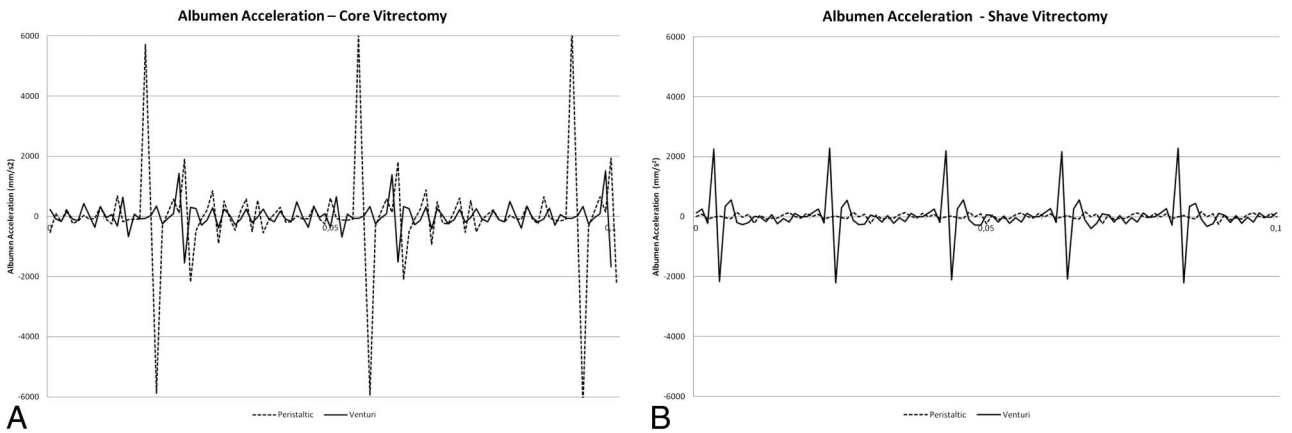

Fig. 9. Acceleration in egg albumen. **A.** *Low-speed* mode at 1,600 cpm and 200 mmHg vacuum. **B.** *High-speed* mode at 3,000 cpm and 300 mmHg vacuum. Acceleration is highly dependent on blade motion and peaks at extremely high levels with the peristaltic pump, although the Venturi pump also produces significantly higher acceleration in albumen than in BSS. In *high-speed*, mode peristaltic pump–induced acceleration lowers significantly.

The use of egg albumen to simulate vitreous is also disputable, although already used in the literature.[19] It retains similar viscosity and, even more importantly, has a fibril structure that accounts for similar rheological behavior while being easier to obtain and less susceptible to time-related deterioration and change of physical and chemical properties than porcine or human vitreous itself.

A more complex scenario that frequently occurs in real-life surgery and we have not been able to simulate is sol–gel mixture. In this case, the cutter port encounters changing medium, and manual parameter adjustment is not possible. Although future generation machines adopting fuzzy logic could conceivably overcome this problem, at present, we can only speculate that volume pumps (such as the peristaltic) should be able to minimize volumetric flow changes better than pressure pumps (such as the Venturi), but the implications on KE and acceleration are much more complex.

In summary, we believe that PIV is a valuable tool and yields important information on velocity, KE, and acceleration of vitreous cutter probes. It also offers a spatial description of fluid perturbation around the cutter probe, allowing precise future comparison of different probes. The clinical relevance of spatial maps is intuitive because every surgeon orientates the cutter probe toward the retina or away from it exactly with the purpose of using or minimizing the field of perturbation induced by the cutter.

Further study is warranted to validate results and develop appropriate measures of fluidics that retain clinical relevance.

Key words: particle image velocimetry, vitreous cutter fluidics, vitreous dynamics, human vitreous motion, pars plana vitrectomy, vitreous acceleration, vitreous velocity.

References

1. Machemer R. Reminiscences after 25 years of pars plana vitrectomy. Am J Ophthalmol 1995;119:505–510.
2. Fujii GY, De Juan E Jr, Humayun MS, et al. A new 25-gauge instrument system for transconjunctival sutureless vitrectomy surgery. Ophthalmology 2002;109:1807–1812.
3. Niu L, Qian M, Wan K, et al. Ultrasonic particle image velocimetry for improved flow gradient imaging: algorithms, methodology and validation. Phys Med Biol 2010;55:2103–2120.
4. Romano GP, Querzoli G, Falchi M. Investigation of vortex dynamics downstream of moving leaflets using robust image velocimetry. Exp Fluids 2010;4:827–838.
5. Rossi T, Querzoli G, Pasqualitto G, et al. Ultrasound imaging velocimetry of the human vitreous. Exp Eye Res 2012;99:98–104.
6. Wals KT, Friberg TR. Vitreous substitute removal rates with the Accurus and Millennium vitrectomy systems. Ophthalmic Surg Lasers Imaging 2008;39:174–176.
7. Pitcher JD III, McCannel CA. Characterization of the fluidic properties of a syringe-based portable vitrectomy device. Retina 2011;31:1759–1764.
8. Falchi M, Querzoli G, Romano GP. Robust evaluation of the dissimilarity between interrogation windows in image velocimetry. Exp Fluids 2006;41:279–293.
9. Fan J, Sheng-Kuei L. Test of significance when data are curves. J Am Stat Assoc 1998;443:1007–1021.
10. Neuhann IM, Hilgers RD, Bartz-Schmidt KU. Intraoperative retinal break formation in 23-/25-gauge vitrectomy versus 20-gauge vitrectomy. Ophthalmologica 2013;229:50–53.
11. Misra A, Ho-Yen G, Burton RL. 23-Gauge sutureless vitrectomy and 20-gauge vitrectomy: a case series comparison. Eye (Lond) 2009;23:1187–1191.
12. Steel DH, Charles S. Vitrectomy fluidics. Ophthalmologica 2011;226:27–35. doi:10.1159/000328207.
13. Magalhaes O Jr, Chong L, DeBoer C, et al. Vitreous dynamics: vitreous flow analysis in 20-, 23-, and 25-gauge cutters. Retina 2008;28:236–241.
14. Fang SY, DeBoer CM, Humayun MS. Performance analysis of new-generation vitreous cutters. Graefes Arch Clin Exp Ophthalmol 2008;246:61–67.
15. Teixeira A, Chong L, Matsuoka N, et al. Novel method to quantify traction in a vitrectomy procedure. Br J Ophthalmol 2010;94:1226–1229.
16. Teixeira A, Chong LP, Matsuoka N, et al. Vitreoretinal traction created by conventional cutters during vitrectomy. Ophthalmology 2010;117:1387–1392.
17. Dugel PU, Zhou J, Abulon DJ, Buboltz DC. Tissue attraction associated with 20-gauge, 23-gauge, and enhanced 25-gauge dual-pneumatic vitrectomy probes. Retina 2012;32:1761–1766.
18. Teixeira A, Chong L, Matsuoka N, et al. An experimental protocol of the model to quantify traction applied to the retina by vitreous cutters. Invest Ophthalmol Vis Sci 2010;51:4181–4186.
19. Wals KT, Friberg TR. Vitreous substitute removal rates with the Accurus and Millennium vitrectomy systems. Ophthalmic Surg Lasers Imaging 2008;39:174–176.